

## **Buckling Behavior of Elastic Kelvin Open-Cell Foams Subjected to Uniaxial Compression**

N. Ohno<sup>1</sup>, D. Okumura<sup>1</sup>, A. Okada<sup>1</sup>

### **Summary**

This paper describes buckling modes and stresses of elastic Kelvin open-cell foams subjected to uniaxial compressions. Cubic unit cells and cell aggregates in model foams are analyzed using a homogenization theory. The analysis is performed on the assumption that the struts in foams have a non-uniform distribution of cross-sectional areas as observed experimentally. By performing the analysis based on the uniformity of strut cross-sectional areas, it is shown that the non-uniformity of cross-sectional areas is an important factor for the buckling behavior of open-cell foams.

### **Introduction**

Gibson and Ashby [1] estimated the buckling collapse strength  $\Sigma_c$  of elastic foams under compression by applying the Euler buckling theory to a cell model consisting of orthogonal struts. They thus analytically derived

$$\Sigma_c = CE_s(\rho_0/\rho_s)^2 \quad (1)$$

where  $C$  is a coefficient,  $E_s$  denotes Young's modulus of the base solid, and  $\rho_0/\rho_s$  indicates the relative density. They showed that Eq. (1) fits experimental results considerably well if  $C \approx 0.05$ , i.e.,

$$\Sigma_c \approx 0.05E_s(\rho_0/\rho_s)^2 \quad (2)$$

The above equation is therefore regarded as an experimentally verified semi-empirical relation.

The cell model of Gibson and Ashby mentioned above has a simple cell morphology that is based on orthogonal struts with identical cross-sectional areas. The cell morphology can be rendered fairly realistic by use of Kelvin's tetrakaidecahedral cells, which are arranged in a body-centered cubic lattice to fill the space. The buckling behavior of elastic Kelvin open-cell foams under compression has been analyzed using finite element methods. One of the findings in the previous studies [2 - 5] is that long wavelength buckling occurs in such open-cell foams subjected to uniaxial compression in the [001] direction, yet the buckling behaviors in other loading directions have not been analyzed. The analysis performed in [3, 6] is regarded as an accurate one, because they took into account the non-uniformity of strut cross-sectional areas observed experimentally [4]. It is then of

---

<sup>1</sup>Department of Computational Science and Engineering, Nagoya University, Japan

interest to discuss the Gibson-Ashby relation (2) in light of the buckling stresses of Kelvin open-cell foams furnished with non-uniform and uniform distributions of strut cross-sectional areas.

In this study, buckling modes and stresses of elastic Kelvin open-cell foams subjected to [001], [011] and [111] uniaxial compressions are analyzed using the updated Lagrangian type two-scale theory [7, 8]. By supposing cubic unit cells and cell aggregates in model foams, the analysis is performed on the assumption that the struts in foams have a non-uniform distribution of cross-sectional areas as observed experimentally [4]. The buckling stresses and modes obtained are then discussed to investigate the dependence on uniaxial compression directions and the influence of strut cross-sectional area distributions.

### Open-Cell Model Foams and Cubic Unit Cells

Fig. 1 illustrates the open-cell model foams analyzed, in which Kelvin's tetrakaidecahedral cells are periodically arranged in a body-centered cubic lattice. The model foams are supposed infinitely large and subjected to uniaxial compression in a direction fixed in the space.

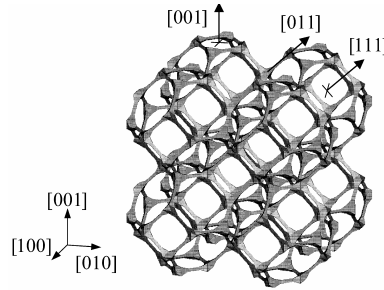


Figure 1: Kelvin open-cell foam and directions of uniaxial compression

The model foams mentioned above have a cubic unit cell  $Y_{cu}$ , shown in Fig. 2(a), owing to the periodicities along [100], [010] and [001] [3, 4, 6]. As seen in Fig. 2(a), a junction is formed by four connecting struts, which have a non-uniform distribution of triangular cross-sectional areas. This kind of junction has been observed experimentally [4]. Figs. 2(b) and 2(c) illustrate the strut-junction connection and their shapes assumed in this study; each strut is expressed using two truncated tetrahedrons and one triangular bar, and each junction is comprised of two regular square pyramids. Then, since one  $Y_{cu}$  contains 24 struts and 24 pyramids, it is shown that the relative density  $\rho_0/\rho_s$  is represented as

$$\rho_0/\rho_s = 8l_{cu}^{-3} \left[ 2^{5/4} A_1^{3/2} + (l_1 - l_2)(A_1 + A_1^{1/2} A_2^{1/2} + A_2) + 3A_2 l_2 \right] \quad (3)$$

where  $l_{cu}$  denotes the size of  $Y_{cu}$ , and  $A_1$ ,  $A_2$ ,  $l_1$  and  $l_2$  are the areas and lengths characterizing the struts (Fig. 2(c)). From now on, the foams with non-uniform

and uniform distributions of strut cross-sectional areas will be referred to as non-uniform and uniform (cross-section) models, respectively.

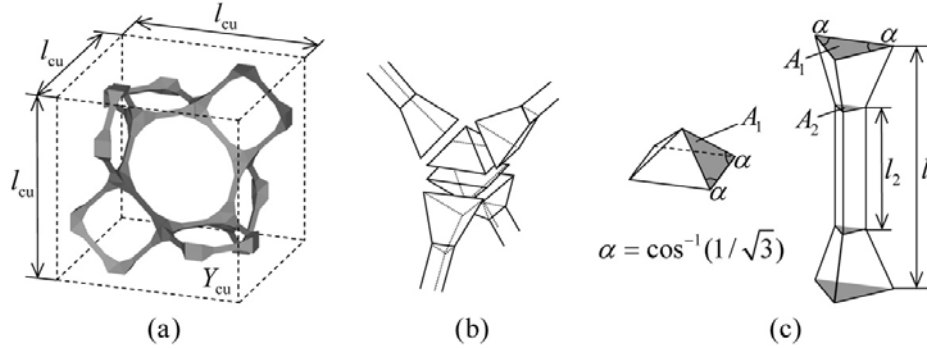


Figure 2: (a) Cubic unit cell  $Y_{cu}$ , (b) strut-junction connection, and (c) shape of struts and junctions

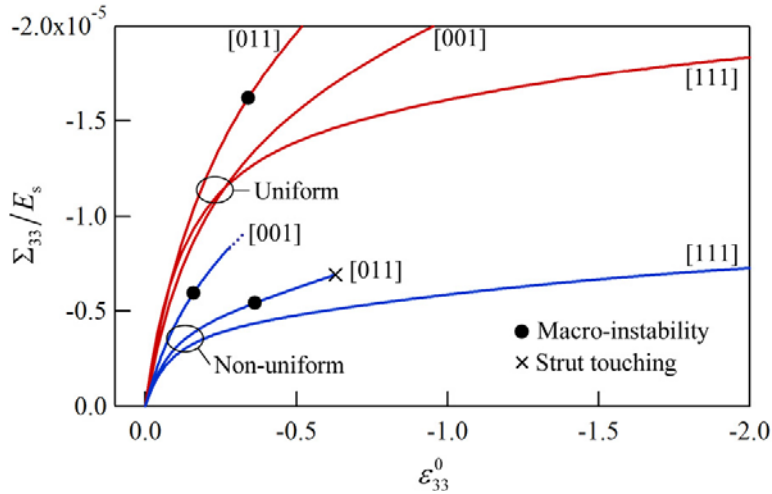


Figure 3: Macroscopic instability points by non-uniform and uniform models of  $\rho_0/\rho_s=0.01$  under [001], [011], and [111] compressions

The values of  $\rho_0/\rho_s$  are taken to be 0.005, 0.010, 0.020, and 0.050 for the non-uniform and uniform models in this study. It is assumed that the non-uniform model has  $l_2/l_1 = 0.5$  and  $A_2/A_1 = 0.15$  based on the experimental measurements [4], while the uniform model has  $A_2/A_1 = 1$ . In the analysis, Young's modulus  $E_s$  of a base solid was employed to non-dimensionalize stresses, and Poisson ratio  $\nu_s$  was taken to be 0.3.

### Macroscopic Instability Analysis

Macroscopic instability was first analyzed to investigate the possibility of long

wavelength buckling using the two-scale theory [7, 8].

Fig. 3 shows the macroscopic instability points found in the macroscopic instability analysis performed for the two models of  $\rho_0/\rho_s = 0.01$ . As seen from the figure, the two models gave quite different results. When the non-uniform model was employed, the macroscopic instability condition was satisfied under [001] and [011] compressions. The uniform model, on the other hand, allowed the condition to be fulfilled only under [011] compression. Macroscopic instability under [011] compression was thus common to the two models. However, the macroscopic instability condition was satisfied much earlier in the non-uniform model than in the uniform model under [011] compression. We therefore can say that the non-uniformity of strut cross sectional areas is an important factor for the stability of open-cell foams.

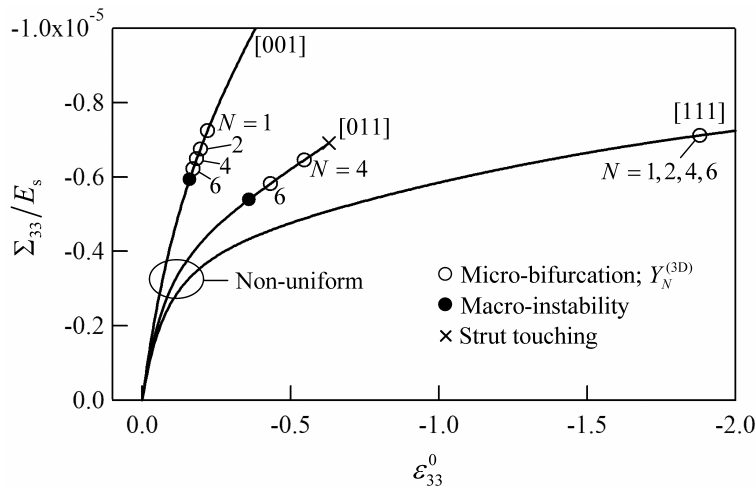


Figure 4: Microscopic bifurcation points determined by use of  $Y_N^{(3D)}$  for non-uniform model of  $\rho_0/\rho_s = 0.01$

Let us remember that macroscopic instability of periodic solids is identified with microscopic bifurcation with an infinitely long wavelength [9]. The results above then suggest that long wavelength buckling can occur in the non-uniform model under [001] and [011] compressions and also in the uniform model under [011] compression.

### Microscopic Bifurcation Analysis

Microscopic bifurcation analysis of the model foams was performed subsequently to the macroscopic instability analysis discussed in the preceding section. Cell aggregates were introduced as periodic units for that bifurcation analysis, because long wavelength buckling was suggested by the macroscopic instability anal-

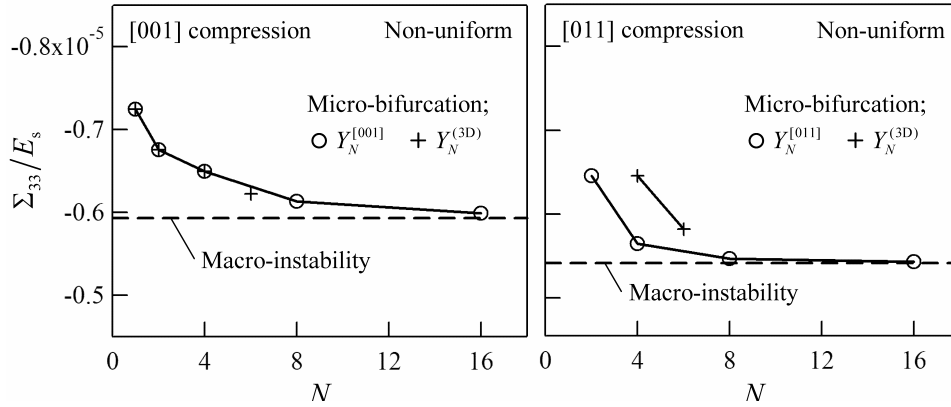


Figure 5: Dependence of microscopic bifurcation stress on the size number  $N$  of periodic units under [001] and [011] compressions; non-uniform model,  $\rho_0/\rho_s = 0.01$

ysis.

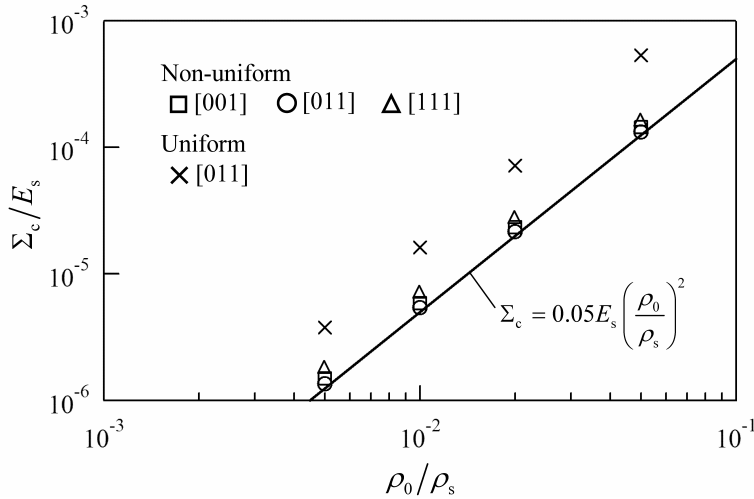


Figure 6: Relation between buckling stress  $\Sigma_c$  and relative density  $\rho_0/\rho_s$ .

The following three types of cell aggregates were employed as periodic units in the microscopic bifurcation analysis:  $Y_N^{(3D)}$ ,  $Y_N^{[001]}$  and  $Y_N^{[011]}$ , which are aggregates of  $Y_{cu}$ . The periodic unit  $Y_N^{(3D)}$  contains  $N^3 Y_{cu}$ s. This periodic unit allows us to find microscopic bifurcation that has the  $k_{[100]}Y_{cu}$  -,  $k_{[010]}Y_{cu}$  - and  $k_{[001]}Y_{cu}$  - periodicities along [100], [010] and [001]. On the other hand,  $Y_N^{[001]}$  and  $Y_N^{[011]}$  are effective for finding microscopic bifurcations that have long wavelengths along [001] and [011], respectively.

The microscopic bifurcation points obtained for the non-uniform model are indicated in Figs. 4 and 5. Under [001] and [011] compressions, the microscopic bifurcation condition was satisfied at lower stresses with increasing number of cells in  $Y_N^{(3D)}$ ,  $Y_N^{[001]}$  and  $Y_N^{[011]}$  (Figs. 4 and 5). The bifurcation stresses provided by  $Y_{16}^{[001]}$  and  $Y_{16}^{[011]}$  were almost equal to the macroscopic instability stresses under [001] and [011] compressions, respectively (Fig. 5). It follows from these results that long wavelength buckling occurred in the non-uniform model under [001] and [011] compressions.

An identical bifurcation point was found under [111] compression using the non-uniform model, though the number of cubic unit cells in  $Y_N^{(3D)}$  was increased from  $N^3 = 1$  to  $6^3$  (Fig. 4). Here it should be recalled that [111] compression led to no macroscopic instability point, suggesting no long wavelength bifurcation (Section 2). It is then clear that the microscopic bifurcation in the non-uniform model under [111] compression had a short wavelength. The buckling behavior of the non-uniform model under [111] compression was thus completely different from those under [001] and [011] compressions.

### Comparison to Gibson-Ashby Relation

As was shown in Sections 3 and 4, macroscopic instability or infinitely long wavelength buckling primarily occurred in the non-uniform model under [001] and [011] compressions and in the uniform model under [011] compression, and only short wavelength buckling happened in the non-uniform model under [111] compression. The buckling stresses determined for these primary buckling modes are plotted against  $\rho_0/\rho_s$  and compared to the Gibson-Ashby relation (2) in Fig. 6. As seen from the figure, the buckling stresses attained in the present analysis provide compressive strength  $\Sigma_c$  with the proportionality to  $E_s(\rho_0/\rho_s)^2$  as expressed in Eq. (1). This implies that the bending of struts is effective for the buckling modes of elastic Kelvin open-cell foams. However, since a simple cell model was employed to derive Eq. (1), the coefficient in this equation was determined by fitting several experiments, as was remarked in Section 1. The resulting equation, Eq. (2), is thus regarded as an experimentally verified semi-empirical relation. As demonstrated in Fig. 6, the primary buckling stresses by the non-uniform model almost satisfy Eq. (2), whereas the uniform model gives a considerable deviation from Eq. (2). We therefore can say that the compressive strength of open-cell foams has been successfully evaluated by analyzing macroscopic instability and short wavelength buckling of the non-uniform model.

### References

1. Gibson, L.J., Ashby, M.F. (1997): *Cellular Solids: Structure and Properties, 2nd Edition*, Cambridge University Press.

2. Laroussi, M., Sab, K., Alaoui, A. (2002): "Foam mechanics: nonlinear response of an elastic 3D-periodic microstructure", *Int. J. Solids Struct.*, Vol. 39, pp. 3599-3623.
3. Gong, L., Kyriakides, S. (2005): "Compressive response of open cell foams - Part II: Initiation and evolution of crushing", *Int. J. Solids Struct.*, Vol. 42, pp. 1381-1399.
4. Gong, L., Kyriakides, S., Jang, W.-Y. (2005a): "Compressive response of open-cell foams. Part I: Morphology and elastic properties", *Int. J. Solids Struct.*, Vol. 42, pp. 1355-1379.
5. Demiray, S., Becker, W., Hohe, J. (2007): "Numerical determination of initial and subsequent yield surfaces of open-celled model foams", *Int. J. Solids Struct.*, Vol. 44, pp. 2093-2108.
6. Gong, L., Kyriakides, S., Triantafyllidis, N. (2005b): "On the stability of Kelvin cell foams under compressive loads", *J. Mech. Phys. Solids*, Vol. 53, pp. 771-794.
7. Ohno, N., Okumura, D., Noguchi, H. (2002): "Microscopic symmetric bifurcation condition of cellular solids based on a homogenization theory of finite deformation", *J. Mech. Phys. Solids*, Vol. 50, pp. 1125-1153.
8. Okumura, D., Ohno, N., Noguchi, H. (2004): "Elastoplastic microscopic bifurcation and post-bifurcation behavior of periodic cellular solids", *J. Mech. Phys. Solids*, Vol. 52, pp. 641-666.
9. Geymonat, G., Müller, S., Triantafyllidis, N. (1993): "Homogenization of nonlinearly elastic-materials, microscopic bifurcation and macroscopic loss of rank-one convexity", *Arch. Ration. Mech. Anal.*, Vol. 122, pp. 231-290.

